CALCULATED X-RAY POWDER DIFFRACTION DATA FOR PHASES ENCOUNTERED IN LEAD/ACID BATTERY PLATES

R. J. HILL

CSIRO Division of Mineral Chemistry, P.O. Box 124, Port Melbourne, Victoria 3207 (Australia)

(Received July 2, 1982)

Summary

Calculated X-ray powder diffraction data are presented, in both graphical and numerical form, for ten phases relevant to the positive and negative plates of the lead/acid battery. The data have been derived from recently published, accurate, single crystal (X-ray) or powder (neutron) diffraction crystal structure studies, and are therefore free from the effects of preferred orientation, phase impurity, micro-absorption, and variation in particle size and shape. Moreover, since the intensities of all possible Bragg reflections consistent with the space group symmetry are calculated, there are no ambiguities in the assignments of the Miller indices of the peaks. The data are given in the form of the complete, simulated Cu Kα diffraction profile from 1 to 100° 2θ (or the first 512 reflections), and also as the integrated intensities relative to a maximum value of 100 for the range 1 - 60° 2θ in each pattern. Calculated Reference Intensity Ratios for the strongest peak in the patterns relative to the (022) reflection of CaF_2 (fluorite) and the (113) reflection of α-Al_2O_3 (corundum), are also presented for use in quantitative X-ray diffraction phase analysis of mixtures of these compounds in lead/acid battery plates.

Introduction

All of the useful energy that can be stored in, or derived from, the lead/acid battery is associated with the so-called "active material" in the positive and negative electrodes (plates). These electrodes usually consist of a lead or lead alloy grid which acts both as a current collector and a support for a paste derived from a mixture of various lead oxides and dilute sulphuric acid. The plates are dried, or "cured", under controlled conditions of temperature and humidity to produce a mixture of lead monoxide and several basic sulphates of lead, and are then immersed in sulphuric acid to receive their first, or "formation", charge. This electrolysis of the cured plates reduces the paste in the negative plate to a sponge-like mass of lead crystals, and oxidizes

0378-7753/83/0000-0000/$03.00

the paste in the positive plate to a mixture of α-PbO_2 and β-PbO_2. Thenceforth, the operation of the battery proceeds according to the thermodynamically reversible reaction

$$\underset{\text{cathode}}{\overset{\oplus}{PbO_2}} + \underset{\text{anode}}{\overset{\ominus}{Pb}} + 2H_2SO_4 \underset{\text{charge}}{\overset{\text{discharge}}{\rightleftharpoons}} \underset{\text{anode}}{\overset{\oplus}{PbSO_4}} + \underset{\text{cathode}}{\overset{\ominus}{PbSO_4}} + 2H_2O \qquad (1)$$

Identification of the reactant and product phases during the above charge and discharge processes, and accurate estimates of the relative abundances and structural states of the phases, are of considerable importance both for quality control during plate manufacture and for determination of the cause(s) of capacity loss and eventual failure during battery operation.

By far the most commonly used method for determining phase identity and abundance is X-ray powder diffraction analysis (XRD). In practice, however, the lead oxide/lead sulphate system does not lend itself easily to XRD methods of analysis because of problems arising from severe peak overlap, high scattering and absorption coefficients, and uncertainty in the degree of crystallinity, the variability of particle size, and the extent of structural distortion [1 - 4].

In spite of these difficulties, the phases occurring in the formed positive plate of the lead/acid battery have been the subject of extensive study by XRD over the last twenty-five years [1, 3, 5 - 17]. By contrast, the formed negative electrode has received much less attention [11, 18], primarily because battery performance has been usually limited by the failure of the positive plates. Some of the XRD studies of the anodic corrosion products of lead and its alloys [6, 19 - 22] are also relevant to the negative plate, although not all of these investigations have been carried out under conditions encountered in the usual operation of lead/acid batteries. However, the complex array of phase transformations that takes place during curing and formation of battery plates has received extensive attention with XRD techniques [18, 23 - 33]. In fact, it has recently been suggested [18] that plates retain a "memory" of their formation procedure and that the history of this treatment determines their subsequent capacity and cycle life.

With a few notable exceptions, these XRD studies have concentrated on the identification of constituent phases, or on the qualitative estimation of changes in phase abundance from changes in the relative intensities of characteristic diffraction peaks. However, phase identification is often a difficult task since many of the basic lead sulphates and lead oxides have similar diffraction patterns, and the samples are often poorly crystalline and/or present with significant preferred orientation. Accurate determination of phase abundance is also difficult since peak intensities are not, in the general case, a simple linear function of phase concentration in multiphase systems [34, 35]. Even in those cases where an attempt has been made to obtain a quantitative determination of the amount of each phase present, either from experimental calibration curves [3, 7, 8, 10, 12, 13] or by the addition of an internal standard [15, 29], the accuracy and precision of the results is

limited by uncertainty associated with the degree of crystallinity, preferred orientation, micro-absorption, extinction, particle size, and lattice distortion of the materials chosen as standards for the analysis.

When present in constant amounts, most of these problems can be effectively "flushed out" of the system by incorporation in the experimentally determined calibration constants. However, when the samples contain nontrivial amounts of non-diffracting (*i.e.*, small crystallite size or "amorphous") material, as documented by a number of workers in the case of the positive plate of the lead/acid battery [12, 13, 15, 36], the amorphous part will contribute to the mass of the phases, but not to the intensity of their diffraction patterns. The carry-over of this effect into the calibration constants can therefore lead to the propagation of errors into all subsequent quantitative analyses.

One approach to the solution of the amorphous material problem is to examine samples of the phase, obtained from different sources, and to use the material with highest crystallinity for the analytical standard [2, 15, 37]. A second approach is to derive the calibration curves from powder diffraction data calculated from the detailed crystal structures of the individual phases [17, 37 - 40]. Since the calculated XRD patterns are based on a model in which the sample is composed of perfectly ordered and randomly oriented crystallites, these patterns are free of preferred orientation, micro-absorption, surface roughness, and amorphous component effects. As well as providing a set of theoretical calibration constants, the calculated patterns may also be used to scrutinize samples prior to analysis while decisions are being made about the technique and internal standard to be used [17]. Moreover, a detailed prior knowledge of the relative intensities of reflections from each phase may also be required to undertake peak "stripping" in mixtures of phases with severe diffraction peak overlap.

In recognition of the important role which can be played by calculated X-ray diffraction patterns in accurate phase identification and analysis, the present paper gives details of the X-ray spectra of ten phases encountered in the plates of lead/acid batteries. The patterns are presented in both a graphical and numerical form, and include a calculation of the "reference intensity ratio" [38, 39] of the strongest peak in each pattern to facilitate quantitative phase analysis of mixtures of the compounds.

Calculation of X-ray powder diffraction patterns

A search of the literature has been made in order to locate data on those phases which are commonly encountered in lead/acid battery plates and for which accurate crystal structure data have been published. The results of this search, together with source data for the standard materials CaF_2 and α-Al_2O_3, are summarized in Table 1. Where the unit cell and/or structure of a compound has been refined more than once, only the more recent and/or more precise data have been included in this Table. The list

TABLE 1

List of compounds studied and the sources of the crystal structure and unit cell data used to generate corresponding X-ray powder diffraction patterns

Compound	Symmetry	Reference source		Comments*
		Crystal structure	Unit cell	
Pb	cubic	[41]	[42]	All atom positions fixed by symmetry. Thermal parameter set equal to 0.5 $Å^2$
α-PbO	tetragonal	[43]	[44]	PND study (R = 0.092). Thermal parameters set equal to β-PbO values
β-PbO	orthorhombic	[45]	[44]	PND study (R' = 0.04)
Pb_3O_4	tetragonal	[46]	[47]	PND study (R = 0.06)
Pb_2O_3	monoclinic	[48]	[48]	PND study (R = 0.041)
α-PbO_2	orthorhombic	[49]	[49]	Full profile PND study (R_B = 0.011). Sample was prepared by oxidation of β-PbO at 340 °C
β-PbO_2	tetragonal	[49]	[49]	Full profile PND study (R_B = 0.023). Univar Analytical Reagent sample
α-2PbO·$PbSO_4$	monoclinic	[50]	[50]	SCXD study (R = 0.07)
PbO·$PbSO_4$	monoclinic	[51]	[51]	SCXD study (R = 0.081)
$PbSO_4$	orthorhombic	[52]	[52]	SCXD study (R = 0.067)
CaF_2	cubic	[41]	[42]	All atom positions fixed by symmetry. Thermal parameters from ref. 53
α-Al_2O_3	rhombohedral	[54]	[54]	SCXD study (R = 0.030)

*PND = powder neutron diffraction; SCXD = single crystal X-ray diffraction; the R values are conventional crystal structure refinement agreement indices.

does not include all of the compounds which have been found in battery plates since the crystal structures of several of the basic lead sulphates (*i.e.*, β-$2PbO \cdot PbSO_4$, $3PbO \cdot PbSO_4$, $3PbO \cdot PbSO_4 \cdot H_2O$, and $4PbO \cdot PbSO_4$ [25, 55 - 59]), the so-called "intermediate oxides" of lead (α-PbO_x and β-PbO_x [60 - 65]), and the basic carbonates of lead ($2PbCO_3 \cdot Pb(OH)_2$ and $6PbCO_3 \cdot 3Pb(OH)_2$ [66 - 68]), have not yet been solved in sufficient detail to allow their patterns to be calculated. Other compounds like $BaSO_4$ and the compounds resulting from the alloy components (Sb, Ca, etc.) of the lead grids, were not considered since they are present in amounts below the detection limit of X-ray powder diffraction analysis.

X-ray powder diffraction patterns have been generated from the structural data referenced in Table 1 using a local version of the Rietveld least-squares structure refinement program [69], modified by Wiles and Young [70] to incorporate the simultaneous treatment of two wavelengths of radiation in a diffractometer. The profiles given in Figs. 1 to 5 were calculated for Cu $K\alpha_1$ (λ = 1.5406 Å) and Cu $K\alpha_2$ (λ = 1.5444 Å) radiation in a Philips diffractometer with fixed slits and no monochromator, and using neutral atom scattering factors, Gaussian peak shapes and a step interval of 0.05° 2θ. The intensity ratio between the α_1 and α_2 wavelengths was taken to be 2:1, and each reflection was assigned a constant full-width at half-peak-height of 0.2° 2θ. The patterns were calculated over the 2θ range 1 - 100° except for those cases where the total number of reflections (α_1 plus α_2) exceeded the program limit of 512, whereupon the upper limit of the pattern was decreased accordingly (*e.g.*, Figs. 3(a), 5(a) and 5(b)). The row of vertical lines below each pattern represents the positions of *all* Bragg reflections allowed by the space group symmetry of the compound, regardless of the value of their calculated intensity.

The reflection intensities given in Tables 2 - 4 were obtained by integration of the $K\alpha_1$ profile data over three half-widths on either side of the reflection centre, and have been presented in a format similar to that used in the JCPDS Powder Diffraction File [42]. The reflection intensities are normalized to yield a maximum value of 100 units, but, in order to limit the Table to manageable proportions, the reflections listed are only those with a *d*-spacing greater than 1.54 Å ($2\theta < 60°$ for Cu $K\alpha$ radiation) and an intensity greater than two units on this scale. The peak positions are indicated by their 2θ value for Cu $K\alpha_1$ radiation, rather than by their *d* spacing, so that a direct comparison can be made with Figs. 1 - 5, and to the corresponding experimental patterns. Since the problem of peak overlap is largely sample- and instrument-dependent, no attempt has been made to combine the reflections into overlapping groups; Figs. 1 - 5 give the complete diffraction patterns under the experimental conditions stated in the legend of Fig. 1. Furthermore, there are no ambiguities in the Miller indices of Tables 2 - 4 since each reflection can be assigned a unique intensity and 2θ value.

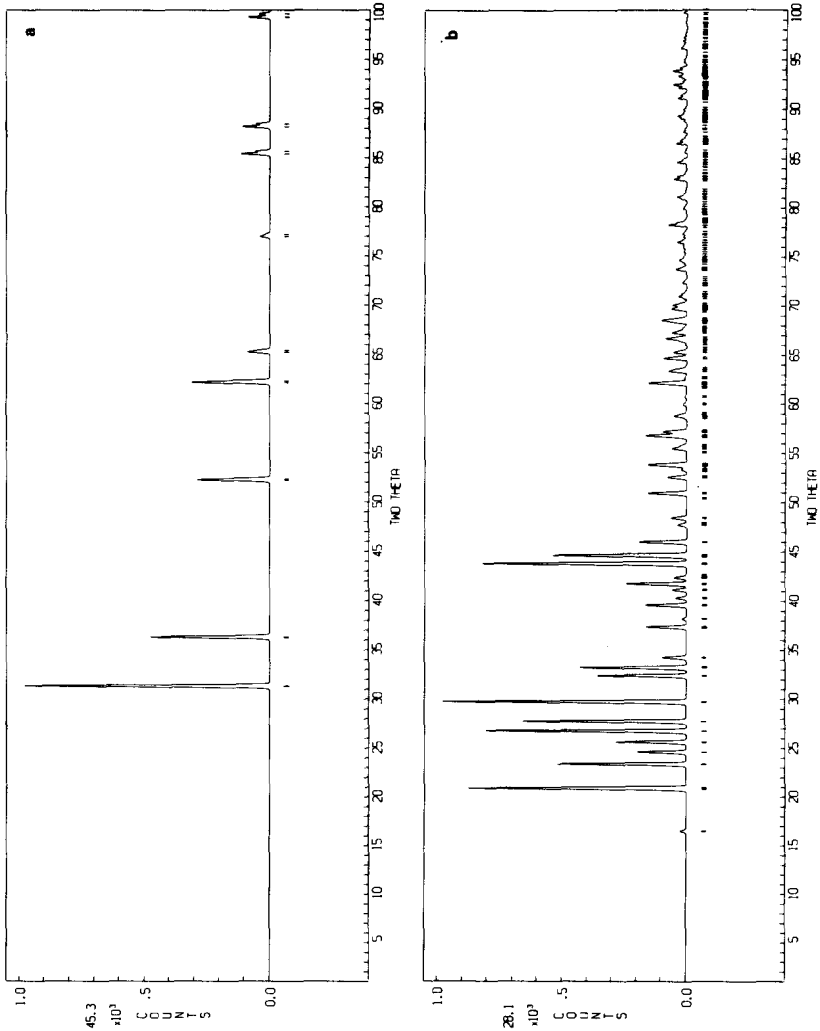

Fig. 1. Calculated X-ray powder diffraction patterns for (a) Pb and (b) $PbSO_4$. The profiles were determined for Cu Kα radiation (λ_{α_1} = 1.5406 Å; λ_{α_2} = 1.5444 Å; $I_{\alpha_1}:I_{\alpha_2}$ = 2:1), using Gaussian peak shapes, and a full-width at half-peak-height of 0.2° 2θ. The row of vertical lines below each pattern represents the positions of all Bragg reflections allowed by the space group symmetry. The unit-cell and atomic-structure parameters used to calculate the pattern were obtained from the references in Table 1.

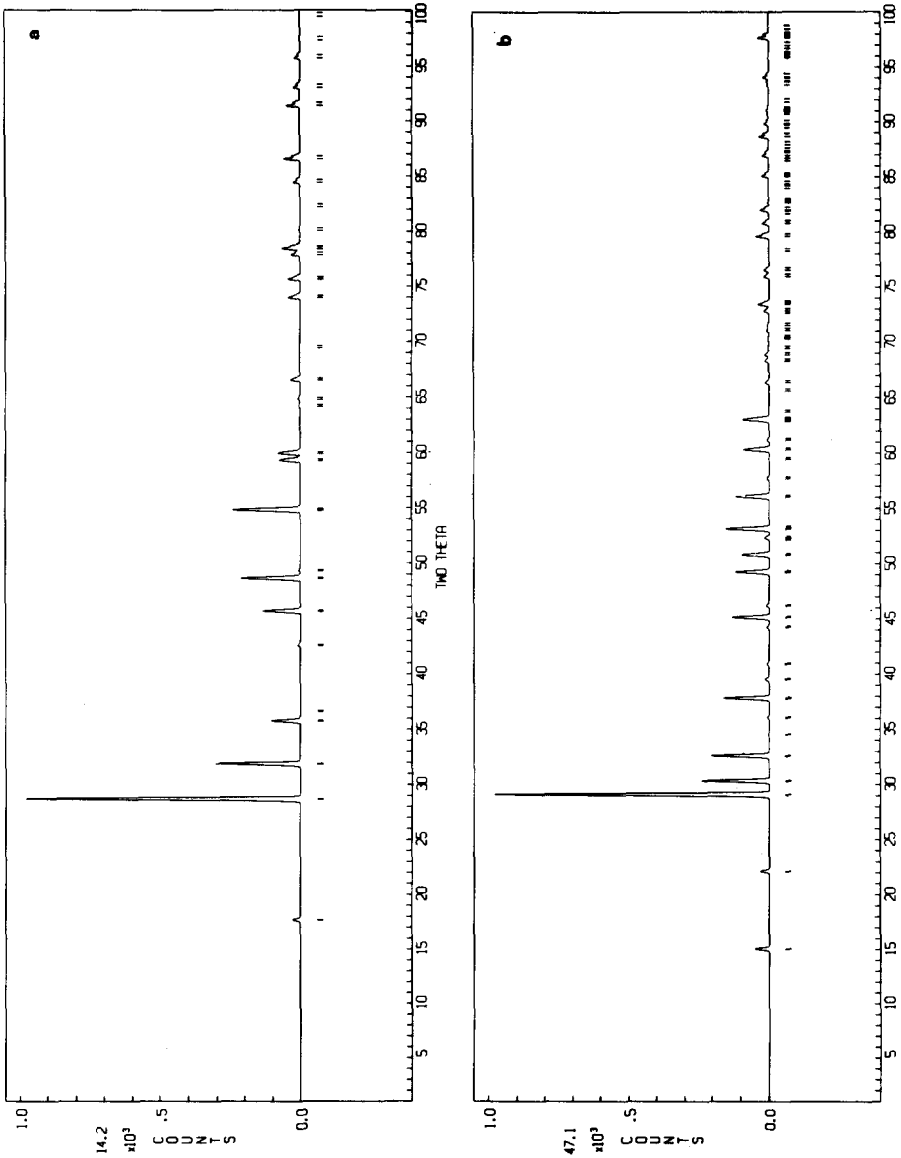

Fig. 2. Calculated X-ray powder diffraction patterns for (a) α-PbO and (b) β-PbO under the conditions outlined in Fig. 1.

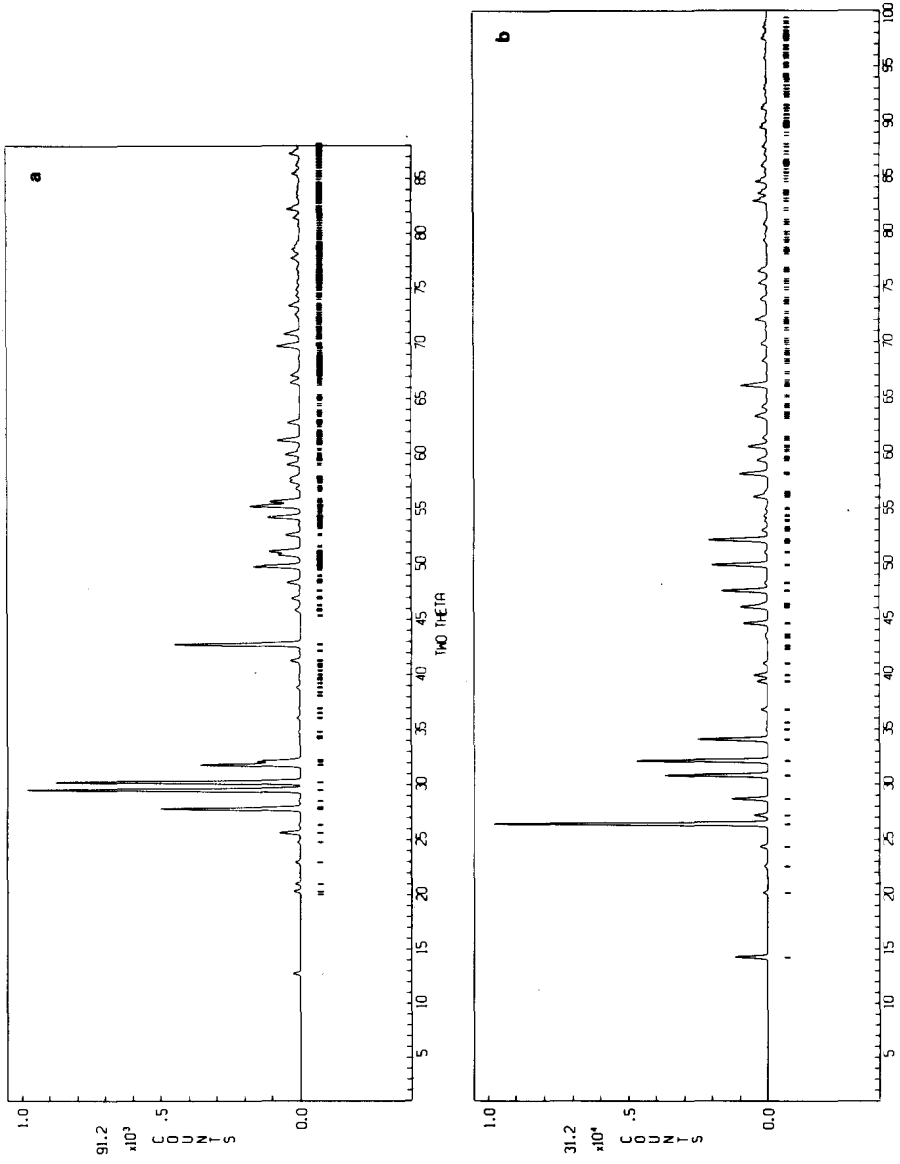

Fig. 3. Calculated X-ray powder diffraction patterns for (a) Pb_2O_3 and (b) Pb_3O_4 under the conditions outlined in Fig. 1.

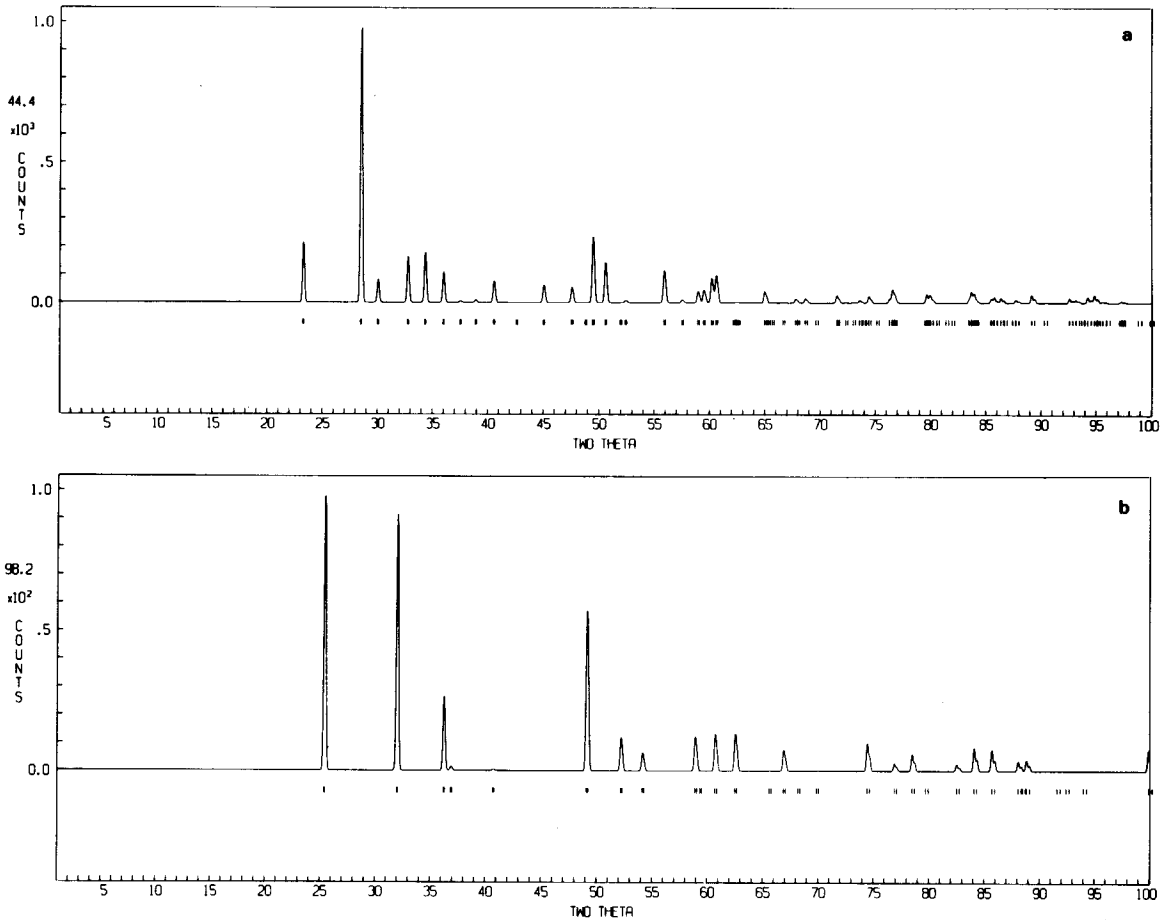

Fig. 4. Calculated X-ray powder diffraction patterns for (a) α-PbO_2 and (b) β-PbO_2 under the conditions outlined in Fig. 1.

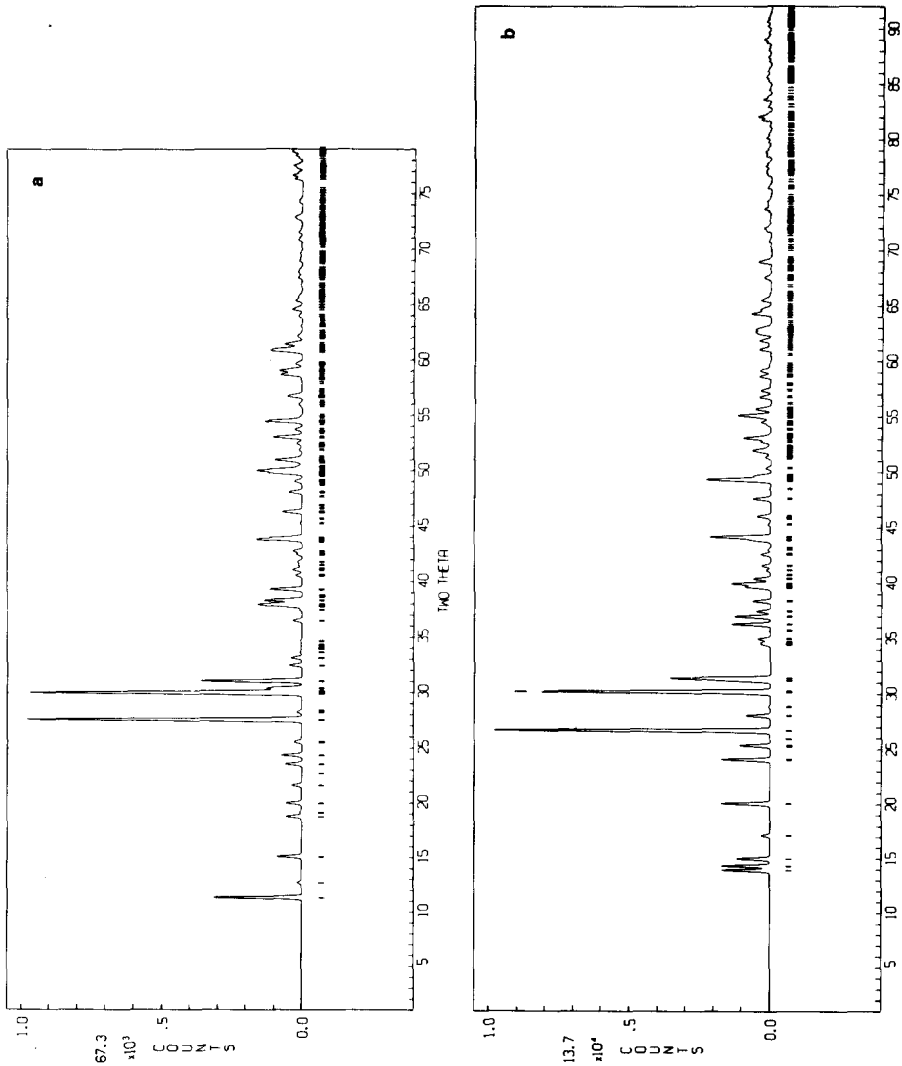

Fig. 5. Calculated X-ray powder diffraction patterns for (a) α-$2PbO \cdot PbSO_4$ and (b) $PbO \cdot PbSO_4$ under the conditions outlined in Fig. 1.

TABLE 2

Calculated X-ray powder diffraction data for Pb, α-PbO and β-PbO (Cu $K\alpha_1$ radiation: 2θ (max) = 60°, I/I_1 (min) = 2.0)

Pb			α-PbO			β-PbO		
2θ (°)	I/I_1	$h\ k\ l$	2θ (°)	I/I_1	$h\ k\ l$	2θ (°)	I/I_1	$h\ k\ l$
31.27	100.0	1 1 1	17.64	2.6	0 0 1	15.03	4.9	1 0 0
36.26	50.3	0 0 2	28.62	100.0	0 1 1	22.12	3.2	1 1 0
52.22	34.6	0 2 2	31.83	31.6	1 1 0	29.08	100.0	1 1 1
			35.72	11.3	0 0 2	30.32	24.9	2 0 0
			45.63	15.7	0 2 0	32.60	21.6	0 2 0
			48.59	25.2	1 1 2	37.81	16.7	0 0 2
			54.76	30.4	1 2 1	45.12	15.0	2 2 0
			59.26	10.0	0 2 2	49.21	12.3	2 0 2
			59.90	10.8	0 1 3	50.77	11.7	0 2 2
						53.10	18.9	3 1 1
						56.03	14.5	1 3 1

TABLE 3

Calculated X-ray powder diffraction data for Pb_3O_4, Pb_2O_3, α-PbO_2 and β-PbO_2 (Cu $K\alpha_1$ radiation: 2θ (max) = 60°, I/I_1 (min) = 2.0)

Pb_3O_4			Pb_2O_3			α-PbO_2			β-PbO_2		
2θ (°)	I/I_1	$h\ k\ l$	2θ (°)	I/I_1	$h\ k\ l$	2θ (°)	I/I_1	$h\ k\ l$	2θ (°)	I/I_1	$h\ k\ l$
14.20	11.3	1 1 0	12.72	2.5	0 0 1	23.25	21.6	1 1 0	25.40	100.0	1 1 0
24.31	2.8	0 2 1	20.29	2.4	0 1 1	28.47	100.0	1 1 1	31.98	95.2	0 1 1
26.35	100.0	1 2 1	25.61	7.5	0 0 2	30.03	8.5	0 2 0	36.23	28.4	0 2 0
27.14	5.1	0 0 2	27.79	50.1	2 0 0	32.74	17.4	0 0 2	49.09	68.1	1 2 1
28.63	13.1	2 2 0	29.49	100.0	2 1 $\bar{2}$	34.30	19.3	0 2 1	52.16	14.7	2 2 0
30.76	37.8	1 1 2	30.20	91.9	0 1 2	35.97	11.6	2 0 0	54.12	8.1	0 0 2
32.09	48.7	1 3 0	31.79	37.5	0 2 0	40.55	8.7	1 1 2	58.88	15.8	1 3 0
34.03	26.2	0 2 2	32.09	15.3	2 1 0	45.02	7.3	0 2 2			
36.74	2.2	2 3 0	32.23	2.2	2 0 $\bar{3}$	47.53	6.5	2 2 0			
39.30	4.2	2 3 1	41.26	3.9	0 2 2	49.43	15.4	2 0 2			
39.86	5.6	2 2 2	42.71	16.9	2 0 $\bar{4}$	49.43	12.6	1 3 0			
44.54	10.1	1 4 1	42.72	33.3	2 2 0	50.55	17.5	2 2 1			
46.02	11.1	2 4 0	46.88	3.1	4 0 $\bar{2}$	55.86	14.6	1 1 3			
47.48	19.0	1 2 3	48.32	5.2	2 0 2	58.92	5.2	2 2 2			
49.81	23.7	0 4 2	49.76	18.6	4 1 $\bar{2}$	59.45	6.0	0 2 3			
52.06	25.5	3 3 2	50.82	8.8	4 0 $\bar{4}$						
52.93	2.3	1 5 0	51.13	12.4	2 1 2						
55.98	6.6	0 0 4	52.62	6.1	0 0 4						
58.04	12.2	2 5 1	54.22	14.5	2 2 $\bar{4}$						
59.27	4.9	4 4 0	55.22	17.1	2 3 $\bar{2}$						
			55.28	5.9	0 1 4						
			55.65	13.2	0 3 2						
			57.40	3.0	4 0 0						
			57.52	2.2	2 1 $\bar{5}$						
			57.76	2.7	4 2 $\bar{2}$						
			59.00	5.6	2 2 2						
			59.91	6.5	4 1 0						

TABLE 4

Calculated X-ray powder diffraction data for α-2PbO·$PbSO_4$, PbO·$PbSO_4$ and $PbSO_4$ (Cu $K\alpha_1$ radiation: 2θ (max) = 60°, I/I_1 (min = 2.0)

α-2PbO·$PbSO_4$			PbO·$PbSO_4$			$PbSO_4$		
2θ (°)	I/I_1	$h\ k\ l$	2θ (°)	I/I_1	$h\ k\ l$	2θ (°)	I/I_1	$h\ k\ l$
11.27	30.9	0 0 1	13.90	16.0	0 0 1	16.46	2.3	1 1 0
15.03	8.7	1 0 $\bar{1}$	14.29	16.1	2 0 0	20.81	72.3	1 0 1
18.69	5.5	1 0 1	14.96	11.3	2 0 $\bar{1}$	20.93	28.4	0 2 0
19.92	5.7	1 1 0	17.12	3.0	1 1 0	23.33	51.1	1 1 1
21.54	3.6	1 1 $\bar{1}$	20.02	16.9	1 1 $\bar{1}$	24.56	19.9	1 2 0
23.47	6.1	1 0 $\bar{2}$	24.02	11.7	2 0 1	25.58	28.0	2 0 0
24.27	7.5	1 1 1	24.04	5.4	1 1 1	26.71	82.5	0 2 1
27.46	100.0	0 1 2	25.31	10.6	3 1 $\bar{1}$	27.69	66.8	2 1 0
29.83	40.6	2 1 0	26.65	100.0	3 1 0	29.68	100.0	1 2 1
29.91	66.7	2 1 $\bar{1}$	28.01	8.7	0 0 2	32.35	37.9	2 1 1
30.08	13.4	2 0 1	30.13	75.0	1 1 $\bar{2}$	33.17	44.1	0 0 2
30.32	12.7	2 0 $\bar{2}$	30.19	23.0	4 0 $\bar{2}$	34.20	9.9	1 3 0
30.97	37.5	0 2 0	31.17	17.3	3 1 $\bar{2}$	37.32	17.5	2 2 1
32.38	4.8	1 1 2	31.37	35.3	0 2 0	39.55	18.5	0 2 2
33.05	3.9	0 2 1	34.63	2.7	2 2 0	40.27	4.8	3 1 0
36.42	3.4	1 2 1	34.93	4.7	2 2 $\bar{1}$	41.10	6.4	2 3 0
37.72	10.0	0 1 3	36.24	14.7	5 1 $\bar{1}$	41.70	27.3	1 2 2
37.91	14.5	2 0 2	36.94	13.6	2 0 2	42.35	5.2	2 0 2
38.24	15.0	2 0 $\bar{3}$	37.42	5.2	4 0 1	43.73	45.3	2 1 2
39.22	8.9	1 2 $\bar{2}$	38.32	6.4	2 0 $\bar{3}$	43.76	50.1	3 1 1
39.23	3.8	1 0 3	39.55	4.6	6 0 $\bar{1}$	44.54	35.1	2 3 1
40.97	3.3	3 1 $\bar{1}$	39.65	5.8	5 1 0	44.64	33.6	1 4 0
42.69	3.6	3 0 1	39.90	14.7	2 2 1	45.95	22.3	0 4 1
43.71	16.5	2 2 1	40.34	6.6	6 0 $\bar{2}$	47.69	3.7	2 2 2
43.89	8.2	2 2 $\bar{2}$	41.52	3.4	3 1 $\bar{3}$	48.38	7.1	1 3 2
46.23	8.4	0 0 4	42.55	3.7	0 2 2	50.88	18.7	3 3 0
48.01	5.6	1 1 $\bar{4}$	43.83	7.5	6 0 0	52.49	7.5	1 0 3
48.96	2.7	3 1 $\bar{3}$	44.10	24.3	4 2 $\bar{2}$	52.56	2.1	4 0 0
49.73	13.5	2 2 2	45.99	5.4	6 0 $\bar{3}$	53.32	2.6	2 4 1
49.99	18.0	2 2 $\bar{3}$	47.56	7.3	5 1 1	53.67	4.2	1 1 3
50.92	2.2	1 0 $\bar{4}$	49.23	14.8	2 2 2	53.74	8.5	4 1 0
50.92	8.4	4 0 $\bar{1}$	49.26	9.9	1 1 $\bar{3}$	53.82	8.2	3 3 1
52.43	2.3	4 0 $\bar{2}$	49.35	5.4	7 1 $\bar{2}$	55.43	6.9	0 2 3
52.97	12.9	0 3 2	49.61	4.6	4 2 1	55.73	2.6	1 5 0
53.67	3.3	3 2 1	49.67	2.3	1 3 $\bar{1}$	56.59	4.1	4 1 1
54.38	5.9	2 3 0	50.33	2.2	2 2 $\bar{3}$	56.72	18.4	1 4 2
54.43	11.2	2 3 $\bar{1}$	51.81	4.4	4 0 $\bar{4}$	57.11	10.7	1 2 3
56.69	6.0	0 2 4	51.97	5.5	6 2 $\bar{2}$	58.74	6.1	2 1 3
58.63	9.3	4 1 1	52.71	4.2	2 0 $\bar{4}$			
59.01	9.9	4 1 $\bar{3}$	53.03	11.5	3 3 0			
59.61	2.2	0 3 3	54.50	3.9	8 0 $\bar{1}$			
			54.89	4.6	6 2 0			
			55.08	12.7	1 3 $\bar{2}$			
			55.61	5.1	5 1 $\bar{4}$			
			55.72	2.4	3 3 $\bar{2}$			
			56.73	5.0	6 2 $\bar{3}$			
			57.32	4.3	1 1 $\bar{4}$			
			58.59	5.1	5 1 2			
			59.06	3.9	5 3 $\bar{1}$			

Calculation of reference intensities

If W_i and I_i are the weight percentage and X-ray intensity, respectively, for a particular reflection (or group of reflections) of phase i in a mixture of n phases, and if W_j and I_j are the corresponding values for a reference phase j, then a quantity RI_{ij} exists [71 - 74] such that:

$$RI_{ij} = (W_j/W_i)(I_i/I_j). \tag{2}$$

The quantity RI is known as the "reference intensity ratio" and is a constant for the particular set of reflections from the two phases when these phases are present in a fixed weight proportion. After determination of the appropriate RI values relative to the reference phase j for all of the phases i in the mixture, then the weight percentages of these phases can be obtained from the so-called direct-comparison, or matrix-flushing, relationship [35, 73, 74]:

$$W_i = (I_i/RI_{ij})[\sum_{i=1}^{n} (I_i/RI_{ij})]^{-1}. \tag{3}$$

Alternatively, if the reference phase j is not normally present in the experimental sample, but has been added in the weight proportion W_j, the weight percentage of any phase i in the mixture can be obtained from the well known internal-standard relationship [34, 35]:

$$W_i = (I_i/I_j)(W_j/RI_{ij}). \tag{4}$$

Values for RI can be obtained by measuring the observed intensities of the reflections from mixtures of known composition, or by calculating the intensities *a priori* from the known crystal structure parameters of each phase. As discussed above, the use of calculated diffraction data offers several advantages in quantitative phase analysis studies. Indeed, the usefulness of a data file of reference intensity ratios has been acknowledged by the JCPDS International Centre for Diffraction Data, firstly by the publication of a file of observed ratios of the peak height of the strongest line of a phase to the strongest line (113) of corundum (α-Al_2O_3) in a 1:1 mixture (by weight) of the two phases, and secondly by the extension of this file to include other reference materials [75].

In our studies of the phase composition of the positive plates of lead/acid batteries it has been demonstrated [17, 76, 77] that CaF_2 is a suitable internal standard for this system. Consequently, reference intensity ratios have been calculated (Table 5) for the most intense peak in each of the 10 battery phases listed in Table 1 relative to the most intense peak (022) of CaF_2 in a 1:1 mixture (by weight), using the expression:

$$RI_{i\,CaF_2} = (Q_i/Q_{CaF_2})(D_{CaF_2}/D_i) \tag{5}$$

where Q is the reflection intensity calculated in ref. 70, and D is the product of the unit cell volume and mass of the unit cell contents (in amu), for each phase. In order to place these reference intensity ratios on a more universal scale, Table 5 also contains RI values for the most intense peak of each phase

TABLE 5

Reference intensity ratios (*RI*), calculated for the strongest reflection in various lead/acid battery phases relative to the (022) reflection of CaF_2 and the (113) reflection of α-Al_2O_3

Compound	Reflection	Reference intensity ratio (*RI*)	
		CaF_2	α-Al_2O_3
Pb	(111)	6.503	26.74
α-PbO	(011)	5.684	23.37
β-PbO	(111)	4.876	20.05 (6.60)*
Pb_3O_4	(12$\bar{1}$)	3.234	13.30
Pb_2O_3	(21$\bar{2}$)	2.318	9.532
α-PbO_2	(111)	4.064	16.71
β-PbO_2	(110)	3.500	14.39
α-2PbO·$PbSO_4$	(012)	1.975	8.121
PbO·$PbSO_4$	(310)	1.857	7.636
$PbSO_4$	(121)	1.038	4.268 (3.50)*
CaF_2	(022)	1.000	4.112 (2.40)*

*Observed *RI* value relative to α-Al_2O_3 obtained from ref. 75.

relative to the (113) peak of the more commonly used internal standard α-Al_2O_3. Note that for certain combinations of these phases the peaks chosen for the reference intensity calculations in Table 5 may be rendered inappropriate by overlap with other peaks. In these cases the reference intensity ratios of other non-overlapping peaks may be calculated using the values in Table 5 in conjunction with the intensity data in Tables 2 - 4.

Discussion and conclusions

With a few notable exceptions [29, 78], published studies of the observed X-ray diffraction profiles of phases encountered in lead/acid batteries are of limited use by themselves, because of the poor crystallinity of the samples, the presence of more than one phase, the limited ranges of diffraction angles and intensities quoted, and/or the absence of exact details of the experimental conditions under which the pattern was collected and the sample was prepared [5, 14 - 16, 19, 22, 33, 57, 65, 79]. When compared with the well defined, calculated XRD patterns in Figs. 1 - 5, the experimental patterns clearly demonstrate problems associated with preferred orientation, particle size distribution, cell dimension changes, small amounts of impurity phases, etc., in the plate samples under study [17, 76, 80].

Similar arguments apply to much of the numerical diffraction data that have been published [2, 25, 44, 56, 57, 78, 81 - 84], including some of the patterns appearing in the JCPDS Powder Diffraction File [75]. For example, the relative peak intensities for α-PbO_2 (card No. 11-549) and α-2PbO·$PbSO_4$

(card No. 22-391) are both in serious error when compared with the data in Tables 3 and 4. In addition, there are many examples of minor indexing mistakes in other patterns which limit their usefulness for quantitative work.

Only three of the calculated reference intensity ratios in Table 5 can be compared with experimental values in the JCPDS Powder Diffraction File [75], and in each case there is very poor agreement. The experimental values are, of course, potentially inaccurate because of the use of peak heights, rather than integrated intensities, and the possible presence of extinction, micro-absorption and preferred orientation, etc. [38, 39]. Indeed, in the case of β-PbO the experimental value is a factor of three too small.

As a check on the calculated and empirical values of *RI* for CaF_2/α-Al_2O_3, a study was made of a 1:1 (by weight) mixture of BDH "extra pure" CaF_2 and Linde A synthetic α-Al_2O_3 of mean particle size 0.3 μm. Using integrated intensities obtained from a diffractometer fitted with a step-scan attachment, an *RI* value of 3.97 was obtained, in good agreement with the calculated value of 4.11 (Table 5). However, the corresponding value based on peak heights was 1.65, even lower than the JCPDS value of 2.40 (Table 5). Results such as these further emphasize the importance both of making comparisons between experimental and calculated data in the assessment of battery materials during X-ray powder diffraction studies, and of using integrated peak intensities and calculated calibration constants in quantitative phase analysis.

Acknowledgements

The author is indebted to the International Lead Zinc Research Organization Inc, for their joint support and for permission to publish this work. All calculations were performed on the CSIRO CYBER 76 computer.

References

1 N. N. Federova, I. A. Aguf, L. M. Levinzon and M. A. Dasoyan, *Ind. Lab.*, *30* (1964) 914.
2 N. E. Bagshaw, R. L. Clark and B. Halliwell, *J. Appl. Chem.*, *16* (1966) 180.
3 D. Kordes, *Chem. Ing. Tech.*, *38* (1966) 638.
4 J. Burbank, A. C. Simon and E. Willihnganz, in P. Delahay and C. W. Tobias (eds.), *Adv. Electrochem. Electrochem. Eng.*, Wiley-Interscience, New York, 1971, p. 157.
5 H. Bode and E. Voss, *Z. Electrokhem.*, *60* (1956) 1053.
6 S. Ikari, S. Yoshizawa and S. Okada, *J. Electrochem. Soc. Jpn.*, *27* (1959) E-186 and E-223.
7 V. H. Dodson, *J. Electrochem. Soc.*, *108* (1961) 401.
8 V. H. Dodson, *J. Electrochem. Soc.*, *108* (1961) 406.
9 W. C. M. Carey, X-ray diffraction as a technique for studying lead–acid battery plates, *Rep. C.R. 21*, July 1965, British Railways Research Department.
10 P. Ness, *Electrochim. Acta*, *12* (1967) 161.
11 T. Chiku, *J. Electrochem. Soc.*, *115* (1968) 982.

12 K. Weisener, W. Hoffmann and O. Rademacher, *Electrochim. Acta, 18* (1973) 913.
13 K. Weisener and P. Reinhardt, *Z. Phys. Chem., 256* (1975) 285.
14 A. A. Abdul Azim and A. A. Ismail, *J. Appl. Electrochem., 7* (1977) 119.
15 P. R. Skidmore and R. R. Schwarz, *Analyst, 104* (1979) 952.
16 H. Nguyen Cong, A. Ejjenne, J. Brenet and P. Faber, *J. Appl. Electrochem., 11* (1981) 373.
17 K. Harris, R. J. Hill and D. A. J. Rand, *J. Power Sources, 8* (1982) 175.
18 D. Pavlov and V. Iliev, *J. Power Sources, 7* (1981/82) 153.
19 P. Ruetschi and B. C. Cahan, *J. Electrochem. Soc., 104* (1957) 406.
20 P. Ruetschi and B. C. Cahan, *J. Electrochem. Soc., 105* (1958) 369.
21 D. Pavlov, *Electrochim. Acta, 23* (1978) 845.
22 F. Arifuku, H. Yoneyama and H. Tamura, *J. Appl. Electrochem., 11* (1981) 357.
23 J. Burbank, *J. Electrochem. Soc., 113* (1966) 10.
24 J. Burbank and E. J. Ritchie, *J. Electrochem. Soc., 116* (1969) 125.
25 H. W. Billhardt, *J. Electrochem. Soc., 117* (1970) 690.
26 D. Pavlov, G. Papazov and V. Iliev, *J. Electrochem. Soc., 119* (1972) 8.
27 D. Pavlov, V. Iliev, G. Papazov and E. Bashtavelova, *J. Electrochem. Soc., 121* (1974) 854.
28 D. Pavlov, *J. Electroanal. Chem., 72* (1976) 319.
29 J. R. Dafler, *J. Electrochem. Soc., 124* (1977) 1312.
30 V. Iliev and D. Pavlov, *J. Appl. Electrochem., 9* (1979) 555.
31 C. F. Yarnell and M. C. Weeks, *J. Electrochem. Soc., 126* (1979) 7.
32 D. Pavlov and G. Papazov, *J. Electrochem. Soc., 127* (1980) 2104.
33 T. G. Chang and M. M. Wright, *J. Electrochem. Soc., 128* (1981) 719.
34 H. P. Klug and L. E. Alexander, *X-ray Diffraction Procedures For Polycrystalline and Amorphous Materials*, Wiley, New York, 1954, p. 410.
35 B. D. Cullity, *Elements of X-ray Diffraction*, Addison-Wesley, Reading, MA, 2nd Edn., 1978, p. 417.
36 S. M. Calder and A. C. Simon, *J. Electrochem. Soc., 121* (1974) 1546.
37 S. Altree-Williams, J. G. Byrnes and B. Jordan, *Analyst, 106* (1981) 69.
38 C. R. Hubbard, E. H. Evans and D. K. Smith, *J. Appl. Crystallogr., 9* (1976) 169.
39 C. R. Hubbard and D. K. Smith, *Adv. X-Ray Anal., 20* (1977) 27.
40 S. Altree-Williams, *Anal. Chem., 50* (1978) 1272.
41 R. W. G. Wyckoff, *Crystal Structures*, Vol. 1. Interscience, New York, 2nd Edn., 1963.
42 *JCPDS International Centre for Diffraction Data 1981, Patterns 4-686 (Pb) and 4-864 (CaF_2).*
43 J. Leciejewicz, *Acta Crystallogr., 14* (1961) 1304.
44 H. E. Swanson and R. K. Fuyat, *Nat. Bur. Stand. (U.S.) Circ. 539*, Vol. II, 1953, p. 30.
45 M. I. Kay, *Acta Crystallogr., 14* (1961) 80.
46 J.-R. Gavarri and D. Weigel, *J. Solid State Chem., 13* (1975) 252.
47 P. Garnier, G. Calvarin and D. Weigel, *J. Solid State Chem., 16* (1976) 55.
48 J. Bouvaist and D. Weigel, *Acta Crystallogr., A26* (1970) 501.
49 R. J. Hill, *Mater. Res. Bull., 17* (1982) 769.
50 K. Sahl, *Z. Kristallogr., 156* (1981) 209.
51 K. Sahl, *Z. Kristallogr., 132* (1970) 99.
52 M. Miyake, I. Minato, H. Morikawa and S. Iwai, *Am. Mineral., 64* (1978) 506.
53 M. J. Cooper and K. D. Rouse, *Acta Crystallogr., A27* (1971) 622.
54 L. W. Finger and R. M. Hazen, *Carnegie Inst. Washington, Yearb. 76* (1976/77) 525.
55 E. V. Margulis and N. I. Kopylov, *Russ. J. Inorg. Chem., 9* (1964) 423.
56 J. D. Esdaile, *J. Electrochem. Soc., 113* (1966) 71.
57 G. Tridot, J. C. Boivin and D. Thomas, *J. Therm. Anal., 1* (1969) 35.
58 H.-J. Kuzel, *Neues Jahrb. Mineral., Monatsh.*, 1973 (1973) 110.
59 R. F. Dapo, *J. Electrochem. Soc., 121* (1974) 253.

60 A. Bystrom, *Ark. Kemi, Mineral. Geol., 20A* (1945) 1.
61 G. Butler and J. L. Copp, *J. Chem. Soc., A*, 1956 (1956) 725.
62 J. S. Anderson and M. Sterns, *J. Inorg. Nucl. Chem., 11* (1959) 272.
63 W. B. White and R. Roy, *J. Am. Ceram. Soc., 47* (1964) 242.
64 J. Bousquet, J. M. Blanchard and B. F. Mentzen, *Bull. Soc. Fr. Mineral. Cristallogr., 94* (1971) 332.
65 C. A. Sorrell, *J. Am. Ceram. Soc., 56* (1973) 613.
66 J. M. Cowley, *Acta Crystallogr., 9* (1956) 391.
67 A. A. Voronova and B. K. Vajnstejn, *Sov. Phys. Crystallogr., 9* (1964) 154 (translated from *Kristallografiya, 9* (1964) 197).
68 J. K. Olby, *J. Inorg. Nucl. Chem., 28* (1966) 2507.
69 H. M. Reitveld, *J. Appl. Crystallogr., 2* (1969) 65.
70 D. B. Wiles and R. A. Young, *J. Appl. Crystallogr., 14* (1981) 149.
71 B. L. Averbach and M. Cohen, *Trans. AIME, 176* (1948) 401.
72 L. E. Alexander and H. P. Klug, *Anal. Chem., 20* (1948) 886.
73 F. H. Chung, *J. Appl. Crystallogr., 7* (1974) 519.
74 F. H. Chung, *J. Appl. Crystallogr., 8* (1975) 17.
75 W. F. McClune (man. ed.), *Powder Diffraction File, Inorganic Phases*, JCPDS International Centre for Diffraction Data, Swarthmore, Pennsylvania, 1981, p. xix.
76 M. T. Frost, J. R. Gardner, J. A. Hamilton, K. Harris, I. Harrowfield, R. J. Hill, J. F. Moresby, D. A. J. Rand, S. Swan and L. B. Zalcman, Prog. Rep. 5: December, 1981, *ILZRO Project No. LE-290.*
77 R. J. Hill, to be published.
78 J. Bouvaist and D. Weigel, *C.R. Acad. Sci., Ser. C, 269* (1969) 486.
79 T. Yagi and S. Akimoto, *Tech. Rep. ISSP*, Ser. A, No. 1024 (1980) 1.
80 J. R. Gardner, K. Harris, R. J. Hill, D. A. J. Rand, S. Swan, R. Woods and L. B. Zalcman, Progress Report No. 3: June, 1982, *NERDDC Project No. 79/9317.*
81 G. Blasse, *Z. Anorg. Allg. Chem., 345* (1966) 222.
82 J.-C. Boivin, D. Thomas and G. Tridot, *C.R. Acad. Sci., Ser. C, 267* (1968) 532.
83 Y. Syono and S. Akimoto, *Mater. Res. Bull., 3* (1968) 153.
84 J. S. White, *Miner. Rec., 1* (1970) 75.